NANO LETTERS

Letter

pubs.acs.org/NanoLett

Probing Absolute Spin Polarization at the Nanoscale

Matthias Eltschka,*[,†] Berthold Jäck,[†] Maximilian Assig,[†] Oleg V. Kondrashov,[‡] Mikhail A. Skvortsov,[§,∥,‡] Markus Etzkorn,[†] Christian R. Ast,[†] and Klaus Kern[†,⊥]

[†]Max-Planck-Institut für Festkörperforschung, 70569 Stuttgart, Germany

[‡]Moscow Institute of Physics and Technology, 141700 Moscow, Russia

[§]Skolkovo Institute of Science and Technology, 143025 Skolkovo, Russia

[∥]L. D. Landau Institute for Theoretical Physics, 142432 Chernogolovka, Russia

[⊥]Institut de Physique de la Matière Condensée, Ecole Polytechnique Fédérale de Lausanne, 1015 Lausanne, Switzerland

Supporting Information

ABSTRACT: Probing absolute values of spin polarization at the nanoscale offers insight into the fundamental mechanisms of spin-dependent transport. Employing the Zeeman splitting in superconducting tips (Meservey–Tedrow–Fulde effect), we introduce a novel spin-polarized scanning tunneling microscopy that combines the probing capability of the absolute values of spin polarization with precise control at the atomic scale. We utilize our novel approach to measure the locally resolved spin polarization of magnetic Co nanoislands on Cu(111). We find that the spin polarization is enhanced by 65% when increasing the width of the tunnel barrier by only 2.3 Å due to the different decay of the electron orbitals into vacuum.

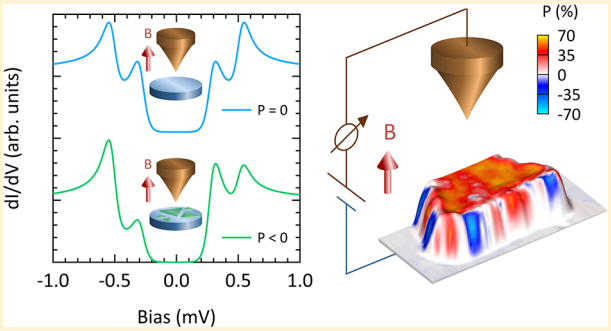

KEYWORDS: *Spin-polarized tunneling, spin-polarized STM, Meservey–Tedrow–Fulde effect, magnetic nanoislands, spin-filtering*

Many modern technological advances such as magnetic hard drives utilize spin-polarized tunnel currents.[1,2] Detecting the spin polarization of tunneling electrons does not only offer insight into the underlying mechanisms of spin-dependent transport but is also essential for novel concepts in spintronics, which employ spin-dependent tunneling on the molecular or even on the atomic scale.[3−7] Here, spin-polarized scanning tunneling microscopy (SP-STM) represents a versatile tool that provides detailed information on the spin properties as well as on the surface topology. In SP-STM, the spin-sensitive signal results from the tunnel magnetoresistance, which in the most simple description is proportional to the product of the local spin polarization of the sample and the tip.[8,9] While SP-STM with (anti)ferromagnetic tips provides information on the relative spin orientation in the sample, direct conclusions concerning the absolute values of spin polarization are difficult due to the unknown electronic structure of the STM tip. However, absolute values are desirable, for example, when comparing the efficiency of multiple spin-dependent transport channels or spin-filter systems at the atomic scale.

For mesoscopic systems such as planar thin film tunnel junctions, the probing capability for absolute spin polarization is provided by the Meservey–Tedrow–Fulde (MTF) effect.[10] In this approach, the detector is a superconductor exposed to magnetic fields. The resulting Zeeman splitting lifts the degeneracy of the quasi-particle density of states (DOS) in the superconductor and opens well-defined spin-up and spin-down channels in the close vicinity of the Fermi level. It is essential that the Zeeman splitting exceeds broadening effects (e.g., thermal broadening) to make the splitting observable (Supporting Information). Therefore, the superconductor is geometrically confined (typically in thin films) to obtain higher critical fields.[10,11] We assume spin conservation during tunneling and a constant DOS in the ferromagnet within the superconducting gap (∼1 meV around the Fermi level).[12] The spin polarization can then be determined on an absolute scale from the observed asymmetry in the differential conductance (dI/dV) spectra[10] because the density of states in the superconductor is known. A major drawback in thin film tunnel junctions is that no local resolution is possible as the measured signal is averaged over the whole area of the tunnel junction. Spin transport is, however, influenced by variations on the atomic scale, and thus, it is desirable to combine the absolute probing capabilities of the MTF effect with the local resolution capabilities of the STM. In addition, as the tunnel barrier of the STM is vacuum, the most ideal barrier, the magnetic structures can be measured directly. This avoids a potential influence of the insulating barrier material on the spin transport through a matching of the electronic structure at the interface or the spin polarizing properties of the barrier material itself.

Received: October 2, 2014
Revised: November 1, 2014
Published: November 25, 2014

   dx.doi.org/10.1021/nl5037947 | *Nano Lett.* 2014, 14, 7171−7174

Here, using superconducting vanadium tips, we transfer the MTF effect to scanning tunneling microscopy (STM) (in the following referred to as MTF-STM) combining the probing capability for absolute spin polarization with precise control at the atomic scale and the well-defined vacuum tunnel barrier of the STM. Since the geometry of an STM tip considerably differs from the well-established thin film superconductors in planar tunnel junctions, it is not a priori clear that tips show the same MTF effect. Nevertheless, we show that the geometrical confinement of a vanadium tip at the apex is well suited to observe the Zeeman splitting for fields up to 4.2 T, which is about an order of magnitude higher than the bulk critical field. To demonstrate the capability of the novel approach, we determine the local spin polarization of bilayer Co nanoislands on Cu(111). We can locally resolve the spin structure of the Co nanoisland with absolute values for the spin polarization. We further find that the spin polarization varies by 65% when changing the tip-to-sample distance by only 2.3 Å, which can be related to a different decay of the spin-up and spin-down wave functions into vacuum.

In Figure 1a, differential conductance (dI/dV) spectra measured with a superconducting V tip on a V(100) single

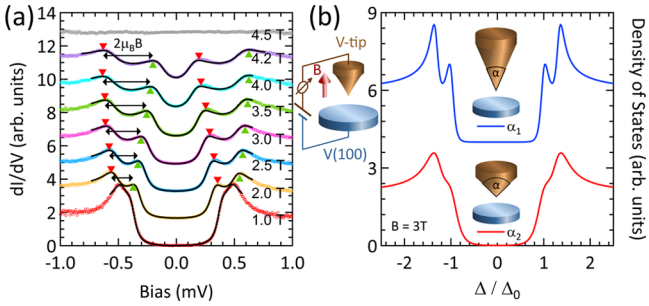

Figure 1. Zeeman splitting in a superconducting STM tip. (a) The dI/dV spectra are measured with a superconducting V tip on normal conducting V(100) at 15 mK. With increasing external magnetic field the Zeeman splitting (indicated by the horizontal arrows) is enhanced and the superconducting gap decreases. The lines are fits based on Maki's theory, red (green) triangles mark the coherence peak of the spin-down (spin-up) channel. (b) Quasi-particle DOS are calculated by Usadel's equation. Larger opening angles α result in spectra with broader features.

crystal (see Supporting Information for preparation details) are presented for increasing out-of-plane magnetic fields. Since the critical field for bulk V is smaller than 0.5 T, the sample is normal conducting for all measurements shown. At our measuring temperature of 15 mK,[13] all spectra feature superconducting quasi-particle DOS for magnetic fields up to 4.2 T, proving that the tip apex remains superconducting. The enhanced critical field results from the confined geometry naturally provided by the tip. The lines in Figure 1a represent fits to the data using a modified Maki equation (Supporting Information).[14,15] The characteristic four-peak-structure of the superconducting coherence peaks is caused by the lifted spin degeneracy of the quasi-particle DOS. The splitting increases with magnetic field B (see arrows in Figure 1a) and follows previous experimental results.[16] This experiment greatly benefits from the choice of V as tip material. Because of its rather low spin−orbit coupling, the spin mixing in a magnetic field is small. Therefore, the resulting spectral features are better separable than in materials with higher spin−orbit coupling. The superconducting gap becomes smaller and closes at the critical field (~4.5 T). Repeating these experiments for several V tips, we observe the same Zeeman splitting in magnetic fields significantly higher than the bulk critical field. The critical fields as well as the superconducting gaps vary for each tip indicating an influence of the tip geometry. To obtain a better understanding of this geometrical influence, we solve a one-dimensional Usadel equation[17] including an external magnetic field and modeling the superconducting tip as a cone with opening angle α. At high magnetic fields, only a small region at the apex of the tip is superconducting. The spectral broadening increases with α (Figure 1b), constituting an intrinsic broadening mechanism particular to the conical shape of the tip. Nevertheless, the Zeeman splitting is still clearly observable.

To demonstrate the capabilities of MTF-STM, we determine the local spin polarization of the well-studied system of bilayer Co nanoislands on Cu(111).[18−23] They are known to be out-of-plane magnetized, i.e., the quantization axis is along the direction of the magnetic field.[19] In Figure 2a, dI/dV spectra

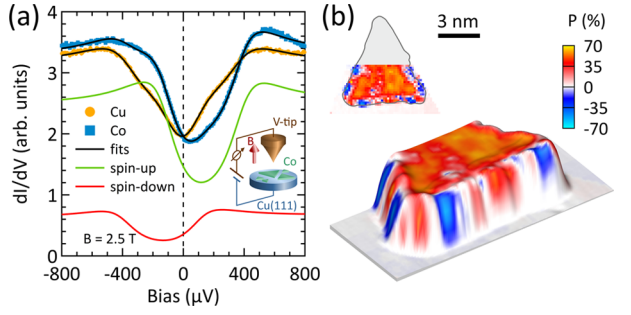

Figure 2. Measurement of spin polarization by MTF-STM. (a) dI/dV spectra are measured on the Cu surface and the Co island with a superconducting STM tip. The spin-up and the spin-down contributions are extracted from the Maki fit of the tunnel spectra acquired on Co. (b) The absolute spin polarization is locally resolved on a Co island.

measured on a Co island and on the Cu surface are shown. On Co, a clear asymmetry in the dI/dV spectra is observed due to the imbalance between the tunneling spin-up and spin-down electrons. We use Maki's theory to fit our spectra because it includes a spin−orbit related mixing of the spin channels in magnetic fields.[14,15] Although the spin−orbit interaction is still rather small, this term needs to be included to minimize the error bar on the extracted spin-polarization (Supporting Information). We use a value $b = 0.14$ in agreement with literature values for V.[24] For the spectra in Figure 2a, we find a high spin polarization of 54 ± 4%. This ability to probe the absolute spin polarization with MTF-STM goes beyond conventional spin-polarized scanning tunneling microscopy (SP-STM), relying on the tunnel magnetoresistance effect between two magnetic electrodes.[9] For the particular superconducting tip shown in Figure 2a, the critical field is lower than in the previous case (~3 T) and the spectral features appear broader, which we attribute to a larger α of the tip apex (Figure 1b). Nevertheless, this does not hamper a detailed analysis of the spin polarization, except for slightly enhanced error bars (Supporting Information).

In order to gain insight into the local variation of spin polarization, we acquire more than 1000 dI/dV spectra on a Co island and extract the map of the absolute spin polarization shown in Figure 2b. Negligible spin polarization ($0\% < P < 2\%$)

dx.doi.org/10.1021/nl5037947 | Nano Lett. 2014, 14, 7171−7174

is obtained on the bare Cu surface meaning that the substrate electrons are not polarized within our error estimation. The inner region of the Co island is governed by the surface state of the majority sp-electrons and shows positive spin polarization. The rim state at the outer region of the Co island is formed by the minority 3d-electrons exhibiting negative spin polarization.[22] These findings, as well as the observed variations within the rim state at the Fermi level, are in good agreement with previous investigations.[19−23] Employing the quantitative scale of MTF-STM, we find negative spin polarization down to −56 ± 5% at the outer region and up to +65 ± 5% around the center position of the Co island. The measured spin polarization is about a factor of 2 higher than the spin polarization above the Co island calculated from density functional theory (DFT).[21,22] This underlines the influence of the tunnel barrier, which we discuss by varying the tip-to-sample distance in the next paragraph.

We find that the spin polarization of the tunneling electrons strongly varies with tip-to-sample distances. dI/dV spectra are acquired on a fixed position in the center of a Co island and on the bare Cu surface for decreasing tip-to-sample distances. The extracted spin polarization is shown in Figure 3a. On Co, the

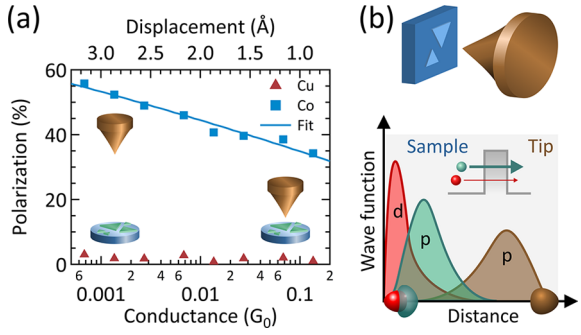

Figure 3. (a) Distance dependence of the spin polarization of tunneling electrons. The spin polarization is measured on a single position of the Co island and the Cu surface for increasing conductance (stabilizing bias voltage V_s = 9.5 mV). The fit shows the spin polarization calculated from a simple 1D model. (b) Schematic illustrations of the orbital wave functions on the spin polarization of tunneling electrons. The specific decay of atomic orbitals is directly correlated with the tunneling probability for the electrons. If the spin states occupy different orbitals, the tunnel current is spin-polarized. Since these electronic orbitals decay differently into vacuum, the spin-polarization of the tunnel current varies with distance.

analysis yields an increase of the spin polarization from 34 ± 3% to 56 ± 5% when the tip-to-sample distance is increased by only 2.3 Å. This corresponds to an increase in spin polarization of 65%. At the same time the conductance decreases from $0.14G_0$ to $0.0007G_0$ where $G_0 = 2e^2/h$ is the conductance quantum. For this measurement range, we emphasize the high sensitivity of the spin-filtering on the barrier width (dP/dz ≈ 10%/Å), which clearly outperforms the benchmark material MgO in its standard range of application.[25]

The strong distance dependence of the spin polarization can be attributed to the specific electronic structure of the Co island because the tip is spin neutral in the sense that the decay of the wave function is independent of the spin. The majority states are mostly formed by the delocalized sp-orbitals of a surface state, while the minority states are governed by localized d-orbitals as shown schematically in Figure 3b.[21,22] The different decay constants of these states into vacuum result in the distance-dependent spin polarization of the tunneling electrons. For a more quantitative analysis, we utilize a simple one-dimensional model to describe the electronic states contributing to the tunnel current I. In our model, the spin polarization is defined as $P = (I_\uparrow - I_\downarrow)/(I_\uparrow + I_\downarrow)$ with the spin-up (↑) and spin-down (↓) contributions of the tunnel current $I_{\uparrow\downarrow} \propto |\langle\psi_{\uparrow\downarrow}|\psi_{tip}\rangle|^2$. Thus, the spin polarization only depends on the overlap of the majority (minority) Co wave function $\psi_\uparrow$ ($\psi_\downarrow$) with ψ_{tip}, the wave function of the tip. The exponential decay of the majority surface state into vacuum is modeled by using the vacuum wave vector $k_0 = (2m_0\Phi/\hbar^2)^{1/2}$ with the free electron mass m_0 and the work function Φ for Co.[26] We also approximate the minority state by an exponential decay; however, we choose the decay constant in such a way as to reproduce the spin polarizations known from DFT calculations (Supporting Information).[21,22] The solid line in Figure 3a represents a fit of this model to the measured distance dependence of the spin polarization of the tunneling electrons. When increasing the tip-to-sample distance the overlap with the localized minority state decreases more quickly than the overlap with the delocalized majority state; hence, the spin polarization of the tunneling electrons increases in very good agreement with the experimental observations. Competing effects such as the change of the tunnel barrier height or trapping states[27−30] are negligible in our measurement setup (Supporting Information).

Transferring the MTF technique to STM, we present a novel approach for probing absolute values of spin polarization at the nanoscale. Because of their confined geometry at the apex, the critical fields of the superconducting V tips are strongly enhanced making the Zeeman splitting of the superconducting quasi-particle DOS observable. Locally resolving the spin polarization of a Co nanoisland shows good agreement with previous studies and adds an absolute scale. The ability to extract the distance dependence in the spin polarization of the tunneling electrons demonstrates the advantages of this new approach. The observed effect can be explained by the difference in the decay length of the spin polarized wave functions of the Co island. This illustrates that access to the absolute spin polarization allows a more fundamental study of the underlying physical mechanism involved in the spin-dependent tunneling process and, therefore, is ideal for comparison with theoretical models. MTF-STM represents an excellent technique to disentangle the contributions of the electrode and barrier material to the spin-polarized tunnel currents. Besides fundamental aspects, our approach offers direct access to a wide variety of systems mimicking components of real devices. For example, the role of metal oxide barriers in spin filters can be investigated on the atomic scale allowing additional information on structural influences, participating electronic wave functions, or the formation of localized states.[30] In novel spintronic devices, our approach provides direct insight into the detailed spin properties on the nanoscale.

■ ASSOCIATED CONTENT

Ⓢ Supporting Information

Meservey−Tedrow−Fulde technique, experimental methods, Maki theory, Usadel equation in the tip, 1D model for Co nanoisland, and distance dependence of the current. This material is available free of charge via the Internet at http://pubs.acs.org.

dx.doi.org/10.1021/nl5037947 | Nano Lett. 2014, 14, 7171−7174

AUTHOR INFORMATION

Corresponding Author
*E-mail: m.eltschka@fkf.mpg.de.

Notes
The authors declare no competing financial interest.

ACKNOWLEDGMENTS

C.R.A. acknowledges funding from the Emmy−Noether Program of the Deutsche Forschungsgemeinschaft (DFG). Research by M.A.S. was supported in part by the program '5top100'.

REFERENCES

(1) Parkin, S. S. P.; Kaiser, C.; Panchula, A.; Rice, P. M.; Hughes, B.; Samant, M.; Yang, S.-H. *Nat. Mater.* **2004**, *3*, 862.
(2) Yuasa, S.; Nagahama, T.; Fukushima, A.; Suzuki, Y.; Ando, K. *Nat. Mater.* **2004**, *3*, 868.
(3) Hirjibehedin, C. F.; Lutz, C. P.; Heinrich, A. J. *Science* **2006**, *312*, 1021−1024.
(4) Khajetoorians, A. A.; Wiebe, J.; Chilian, B.; Wiesendanger, R. *Science* **2011**, *332*, 1062−1064.
(5) Miyamachi, T.; et al. *Nature* **2013**, *503*, 242.
(6) Raman, K. V.; Kamerbeek, A. M.; Mukherjee, A.; Atodiresei, N.; Sen, T. K.; Lazić, P.; Caciuc, V.; Michel, R.; Stalke, D.; Mandal, S. K.; Blügel, S.; Münzenberg, M.; Moodera, J. S. *Nature* **2013**, *493*, 509.
(7) von Bergmann, K.; Ternes, M.; Loth, S.; Lutz, C. P.; Heinrich, A. J. *ArXiv* **2014**, 14108767.
(8) Jullière, M. *Phys. Lett. A* **1975**, *54*, 225−226.
(9) Wiesendanger, R. *Rev. Mod. Phys.* **2009**, *81*, 1495−1550.
(10) Meservey, R.; Tedrow, P. M. *Phys. Rep.* **1994**, *238*, 173−243.
(11) Suderow, H.; Bascones, E.; Izquierdo, A.; Guinea, F.; Vieira, S. *Phys. Rev. B* **2002**, *65*, 100519.
(12) Tedrow, P. M.; Meservey, R. *Phys. Rev. Lett.* **1971**, *27*, 919−921.
(13) Assig, M.; Etzkorn, M.; Enders, A.; Stiepany, W.; Ast, C. R.; Kern, K. *Rev. Sci. Instrum.* **2013**, *84*, 033903.
(14) Maki, K. *Prog. Theor. Phys.* **1964**, *32*, 29.
(15) Worledge, D. C.; Geballe, T. H. *Phys. Rev. B* **2000**, *62*, 447−451.
(16) Gibson, G. A.; Meservey, R. *Phys. Rev. B* **1989**, *40*, 8705−8713.
(17) Usadel, K. D. *Phys. Rev. Lett.* **1970**, *25*, 507−509.
(18) Diekhöner, L.; Schneider, M. A.; Baranov, A. N.; Stepanyuk, V. S.; Bruno, P.; Kern, K. *Phys. Rev. Lett.* **2003**, *90*, 236801.
(19) Pietzsch, O.; Kubetzka, A.; Bode, M.; Wiesendanger, R. *Phys. Rev. Lett.* **2004**, *92*, 057202.
(20) Pietzsch, O.; Okatov, S.; Kubetzka, A.; Bode, M.; Heinze, S.; Lichtenstein, A.; Wiesendanger, R. *Phys. Rev. Lett.* **2006**, *96*, 237203.
(21) Niebergall, L.; Stepanyuk, V. S.; Berakdar, J.; Bruno, P. *Phys. Rev. Lett.* **2006**, *96*, 127204.
(22) Oka, H.; Ignatiev, P. A.; Wedekind, S.; Rodary, G.; Niebergall, L.; Stepanyuk, V. S.; Sander, D.; Kirschner, J. *Science* **2010**, *327*, 843−846.
(23) Oka, H.; Tao, K.; Wedekind, S.; Rodary, G.; Stepanyuk, V. S.; Sander, D.; Kirschner, J. *Phys. Rev. Lett.* **2011**, *107*, 187201.
(24) Tedrow, P.; Meservey, R. *Phys. Lett. A* **1978**, *69*, 285−286.
(25) Butler, W. H.; Zhang, X.-G.; Schulthess, T. C.; MacLaren, J. M. *Phys. Rev. B* **2001**, *63*, 054416.
(26) Davison, S. G.; Steslicka, M. *Basic Theory of Surface States*; Clarendon Press: Gloucestershire, U.K., 1996.
(27) Slonczewski, J. C. *Phys. Rev. B* **1989**, *39*, 6995.
(28) Gimzewski, J. K.; Möller, R. *Phys. Rev. B* **1987**, *36*, 1284.
(29) Ding, H. F.; Wulfhekel, W.; Schlickum, U.; Kirschner, J. *Europhys. Lett.* **2003**, *63*, 419.
(30) Wang, K.; Levy, P. M.; Zhang, S.; Szunyogh, L. *Philos. Mag.* **2003**, *83*, 1255−1286.